Polar study of ionospheric ion outflow versus energy input

Yihua Zheng,[1] Thomas E. Moore,[2] Forrest S. Mozer,[3] Christopher T. Russell,[4] and Robert J. Strangeway[4]

Received 27 December 2004; revised 4 March 2005; accepted 8 April 2005; published 9 July 2005.

[1] A statistical study of the ion outflow versus energy input is performed by using multi-instrument data (TIDE, EFI, MFI, HYDRA) from Polar during its perigee auroral passes in the year 2000. Several important physical quantities connected to the ion outflow have been investigated, including the Poynting flux from the perturbation fields (below 1/6 Hz), the electron density, temperature, and the electron energy flux. The perturbation fields used here to calculate the Poynting flux may be associated with the small-scale quasi-static field structures of the field-aligned currents or/and the very low frequency Alfvén waves (below 1/6 Hz), which are both proven to be important energy sources for powering the aurora. Our results show that the field-aligned ion outflow flux correlates best with the Earth-directed Poynting flux and the precipitating electron density and also demonstrates almost no correlation with the electron energy flux and temperature. The findings from this Polar study are similar to those from FAST. The general corroboration between the independent data sets of the two spacecraft suggests that the empirical ion outflow scaling laws can be established, which will be beneficial to global simulation efforts. Our results show that at 6000 km altitudes $f_i = 10^{6.836\pm0.028}S^{0.535\pm0.086}$ and $f_i = 10^{6.650\pm0.063}n_e^{0.484\pm0.147}$, where f_i is the total field-aligned ion outflow flux in $1/cm^2/s$, S is the Poynting flux in $ergs/cm^2/s$, and n_e is the electron density in $1/cm^3$.

Citation: Zheng, Y., T. E. Moore, F. S. Mozer, C. T. Russell, and R. J. Strangeway (2005), Polar study of ionospheric ion outflow versus energy input, *J. Geophys. Res.*, *110*, A07210, doi:10.1029/2004JA010995.

1. Introduction

[2] Ionospheric ion outflows play a very important role in magnetosphere-ionosphere coupling. These flows possibly provide a significant particle source for populating the inner magnetosphere and the nightside plasma sheet [*Chappell et al.*, 1987, 2000; *Moore*, 1991; *Moore and Delcourt*, 1995; *Winglee*, 1998] and even have potential global impacts for the entire Sun-Earth system through plasma transport, magnetospheric convection, and via their influences on the onset of magnetic reconnection at both dayside and nightside [*Chen and Moore*, 2004; *Moore et al.*, 1999; *Winglee et al.*, 2002; *Winglee*, 2004].

[3] Over 4 decades of research have unveiled many aspects of ionospheric ion outflows. It is known that ion outflows from Earth's ionosphere into its magnetosphere are highly variable in composition, energy, space, and time. Statistical analysis of in situ observations has demonstrated that ion outflow is solar cycle [*Yau et al.*, 1985], seasonal [*Collin et al.*, 1998], and geomagnetic activity dependent [*Yau et al.*, 1985]. The association of ionospheric outflow mass flux enhancements with solar EUV activity ($F_{10.7}$, the 10.7 cm microwave flux as solar EUV proxy) has been shown to result from the enhancement of neutral oxygen (O) density in the topside ionosphere, at the expense of the neutral hydrogen (H) density [*Cannata and Gombosi*, 1989]. The association with *Kp* index suggests a relationship of ion outflows with nightside auroral activity. A good correlation has been reported between the occurrence frequency of dayside ion upwelling and the solar wind dynamic pressure [*Giles*, 1993]. In a survey of cleft ion outflows performed by *Pollock et al.* [1990], a close association with the field-aligned currents was found. However, no significant correlation was found between the interplanetary magnetic field (B_z) and the upwelling plasma flux. The response of ionospheric ion outflows to the solar and solar wind driver, such as coronal mass ejection (CME)-induced shocks, can be prompt as shown by *Moore et al.* [1999] and *Fuselier et al.* [2001].

[4] The upward ion motion along the geomagnetic field lines in the high-latitude ionosphere can be divided into two major categories, as stated by *Yau and André* [1997]: bulk ion flows with energies up to a few eV in which all the ions acquire a bulk flow velocity and ion energization processes in which only a fraction of ions are energized but to much higher energies. The former category includes polar wind and auroral bulk ion outflow. The latter includes transversely accelerated ions, upwelling ions, ion conics, and beams. In order for the collisional lower ionospheric ions with average energies of 0.1 eV to reach escape velocity, their energy must be increased at least to about 1 to 10 eV (for H+ and O+,

[1]Johns Hopkins University Applied Physics Laboratory, Laurel, Maryland, USA.
[2]Laboratory for Extraterrestrial Physics, NASA Goddard Space Flight Center, Greenbelt, Maryland, USA.
[3]Space Science Laboratory, University of California, Berkeley, California, USA.
[4]Institute of Geophysics and Planetary Physics, University of California, Los Angeles, California, USA.

0148-0227/05/2004JA010995$09.00

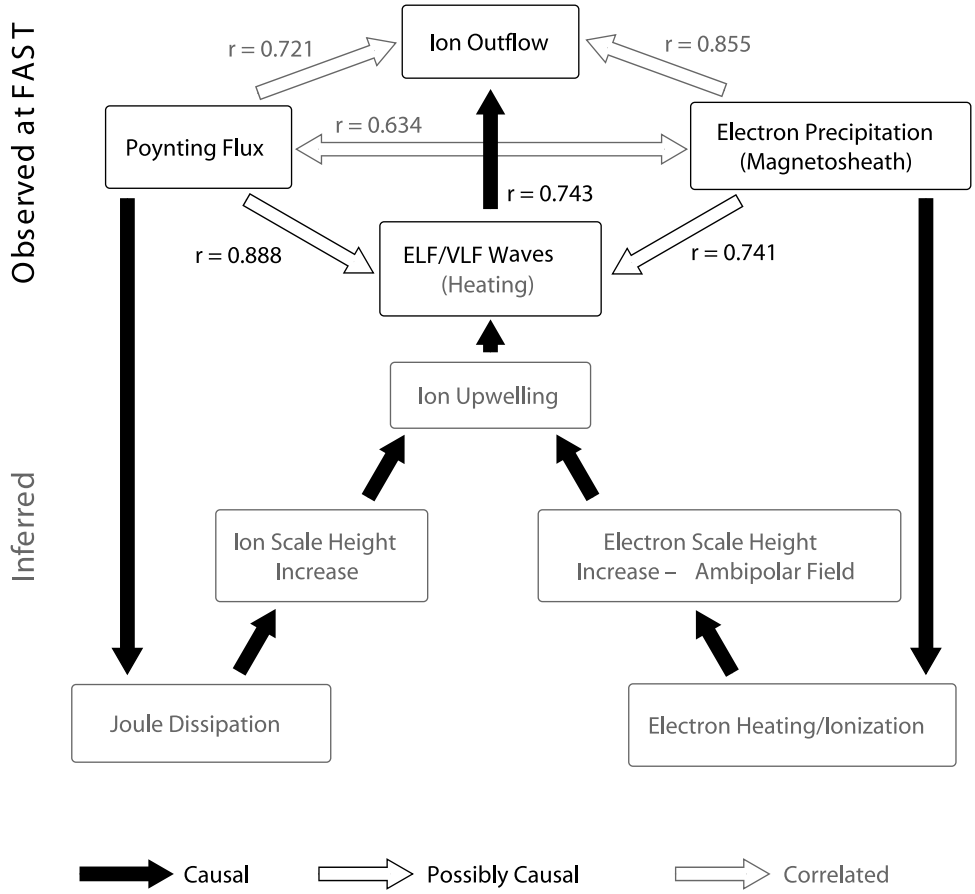

Figure 1. A diagram showing various controlling factors of ionospheric ion outflow, the interrelationship among the physical quantities and the ion outflow mechanisms (from *Strangeway et al.* [2005]).

respectively), possibly by gradual energization as they move upward. More than one ion energization mechanism can be at work within each category, and a combination of all is important for the total ion outflow. The energization mechanisms that cause heavy ion outflows can be ordered into two major categories: parallel and perpendicular acceleration/heating. Some of them are topside frictional heating; transverse acceleration/heating by low-frequency waves at higher altitudes, where the collisional frequency falls below the gyrofrequency; and parallel acceleration/heating, where the parallel electric field is enhanced or there is existence of parallel potential drops.

[5] Although the ultimate source of energy that drives heavy ion outflow in the ionosphere is the solar wind, the Earth's magnetosphere, as the linkage between the Sun and the ionosphere, therefore serves an important role in the energy transfer from the Sun to the ionosphere. In the magnetosphere-ionosphere coupling, the magnetosphere delivers energy to the high-latitude ionosphere in the form of precipitating electrons/ions, field-aligned currents, or low-frequency waves such as Alfvén waves. Despite the great progress made in the research of ion outflow and its various energization mechanisms, little has been done in correlating ion outflow with its different energy inputs [*Strangeway et al.*, 2005]. In *Strangeway et al.*'s [2005] study of ion outflow versus energy inflow using FAST data, electron precipitation was found to be the strongest average controlling factor of the outflow. Although Alfvén waves come as the second most important factor, there is no shortage of evidence of their capability in enhancing electron precipitation and their contribution to the ion outflow [e.g., *Su et al.*, 2001; *Chaston et al.*, 1999, 2003; *Tung et al.*, 2001]. A summary of his results is illustrated in Figure 1. To complement Strangeway's study, we perform a similar statistical study, by using multi-instrument data from Polar during its auroral perigee passes in the year 2000, on the relationship between the auroral ion outflow and its various local controlling factors, particularly on the heavy ions. The Poynting flux due to the perturbed fields and several parameters of the precipitating electrons were extracted from the data to examine their association with the total ion outflow. Work of this kind not only can help us with a better understanding of the relative importance of different energy inputs and the ion outflow mechanisms but it can also help the global simulation community set the right constraints for the boundary condition and eventually realize the ultimate goal of creating and utilizing a self-consistent outflow model within the Global Geospace Circulation Model (GGCM).

[6] This paper is organized as follows: Section 2 presents the methodology of the data analysis and the statistical

results. Discussion is given in section 3 and conclusion is provided in section 4.

2. Data Analysis Methodology and Statistical Results

2.1. Database Compilation

[7] In order to correlate the ion outflow flux with the Poynting flux and several parameters of the precipitating electrons, data from multiple instruments of POLAR have to be utilized. POLAR was launched on 24 February 1996 into a 1.8 × 8.9 R_E polar orbit with a period of about 18 hours. Here we use TIDE (STOPS) (Thermal Ion Dynamics Experiment) [*Moore et al.*, 1995] for the ion outflow flux calculation and HYDRA [*Scudder et al.*, 1995] for the electron measurements. Fields data are from EFI (Electric Field Instrument) [*Harvey et al.*, 1995] and MFE (Magnetic Field Experiment) [*Russell et al.*, 1995]. To compile the database, we first went through all of the perigee passes (with altitude ~4000–~6000 km in the southern hemisphere) of POLAR during the year 2000 to locate the ion outflow events using TIDE data. (The year 2000 was chosen in part owing to the availability of all the data concerned at the time of database assembly and in part owing to its proximity to the solar maximum epoch.) On the basis of the list of the ion outflow events, we then checked whether data from the other instruments of interest (HYDRA, EFI, and MFE) were available as well. In total, 37 events of the year 2000 were found, comprising the database for this study.

2.2. Example Event and Key Physical Parameters

[8] A typical example (2 January 2000) of the ion outflow events in the database is provided in Figure 2. The top four parts are the thermal ion measurements obtained from TIDE and the bottom four parts are the electron data from HYDRA. Shown from top to bottom are TIDE spin angle-time spectrogram, energy-time spectrogram, TIDE ion density, TIDE ion velocity along the magnetic field, electron density, electron mean energy, electron energy-time spectrogram antiparallel to the magnetic field, and the electron energy-time spectrogram including all pitch angles, respectively.

[9] TIDE measures the velocity distribution of ions once per 6-s spin of the spacecraft. It samples nearly the entire sky at a nominal resolution of 22.5° (polar angle) by 11.25° (spin azimuth angle) and in the energy range from 0.3 to ~400 eV with resolution $\Delta E/E \sim 0.25$. TIDE was built with a time-of-flight (TOF) mass analyzer capable of sorting ions according to its species. The TOF system has two components: STARTS and STOPS, which can detect the speed of each detected particle via the time recordings at the two components (given the distance between the two). Known energy per charge, the mass per charge of the particle is therefore determined. However, in this study, only the STOPS component of TIDE data is used because the STARTS component has not been available since late 1996.

[10] The spin angle–time spectrogram in Figure 2a shows the time evolution of the number fluxes in all spin azimuth angles summed over all 31 energy channels. The plus and minus symbols are used to indicate the parallel and the antiparallel directions (relative to **B**) in Figure 2a. The cross symbol is the ram direction. The magnetic field during the perigee passes is outward because the spacecraft was located at southern hemisphere during such times. Figure 2b shows the energy-time spectrogram summed over all spin angles for each of the energy channel. The colors in Figures 2a and 2b are used to indicate the logarithmic value of the number flux in the unit of log [cm^{-2} s^{-1} sr^{-1} eV^{-1}]. From Figures 2a and 2b, we can see that this is a tangential pass through the noon cusp region, around the highest latitude of the orbit. The observed ion spectrograms during 1615–1622 UT appear to be superposition of two populations: ''cold'' ions at a few eV (presumably O+) in the ram direction and ''hot'' isotropic hundred eV ions (presumably H+). There was considerable thermal O+ shift from the ram direction (the cross symbol in Figure 2a) during the interval of 1624–1632 UT, coincident with the large earthward flowing Poynting flux shown in Figure 3. The electron density in Figure 2e and the mean electron energy in Figure 2f are two key parameters from HYDRA. The electron density here is only a partial electron density obtained between a low-energy cutoff and a higher-energy cutoff. Figure 2 illustrates that there is a good correlation between ionospheric ion outflow and soft electron (<1 keV) precipitation, demonstrating that our study can complement what was found with FAST data [*Strangeway et al.*, 2005]. The good correlation between the ionospheric ion outflow and soft electron precipitation is also consistent with the model results of *Liu et al.* [1995].

[11] Figure 3 shows the event time series for 2 January 2000. Figure 3a shows the spacecraft potential in volts from EFI. Figures 3b to 3e are the perturbed electric field and magnetic field in the two perpendicular directions with ''o'' in the direction of $\mathbf{B} \times (\mathbf{B} \times \mathbf{r})$ and ''e'' in the direction of $\mathbf{B} \times \mathbf{r}$ (where $\mathbf{r}$ is the position vector of the spacecraft). The perturbation magnetic field d**B** is the measured magnetic field from MFE, deducted by the T96 model field under the nominal condition (with the solar wind dynamic pressure = 2 nPa, IMF $B_y = B_z = 0$, and Dst = 0). Both the magnetic field and the electric field used are at 6 s resolution. A filter with the frequency band of [1/600–1/6 Hz] is applied to the calculation of Poynting flux used in this study. Figure 3f shows the Poynting flux (derived from Figures 3b–3e) along the magnetic field in ergs/cm^2/s with negative values meaning the electromagnetic energy flux going earthward. Figure 3g is the magnetic field-aligned total ion number flux obtained from TIDE in #/cm^2/s, with positive values indicating outflowing ions. Figure 3h shows the absolute value of total ion outflow number flux in logarithmic value, with grey triangles representing outflowing ion flux and black stars representing incoming ion flux. The field-aligned total ion number flux is calculated from the TIDE measurement and O+ is the major contributor to it. To circumvent the lack of mass discrimination ability, special efforts were made to calculate the field-aligned total ion number flux directly from the original measurements (counts per second), with only gyrotropy around the magnetic field assumed.

[12] The hydra electron data were obtained from CDAWEB with the electron density and temperature at ~1 min (55.2 s) resolution and electron differential energy fluxes at 13.8 s resolution. From the electron density and the temperature, we can get the electron pressure. Another quantity which we correlated with the total ion outflow

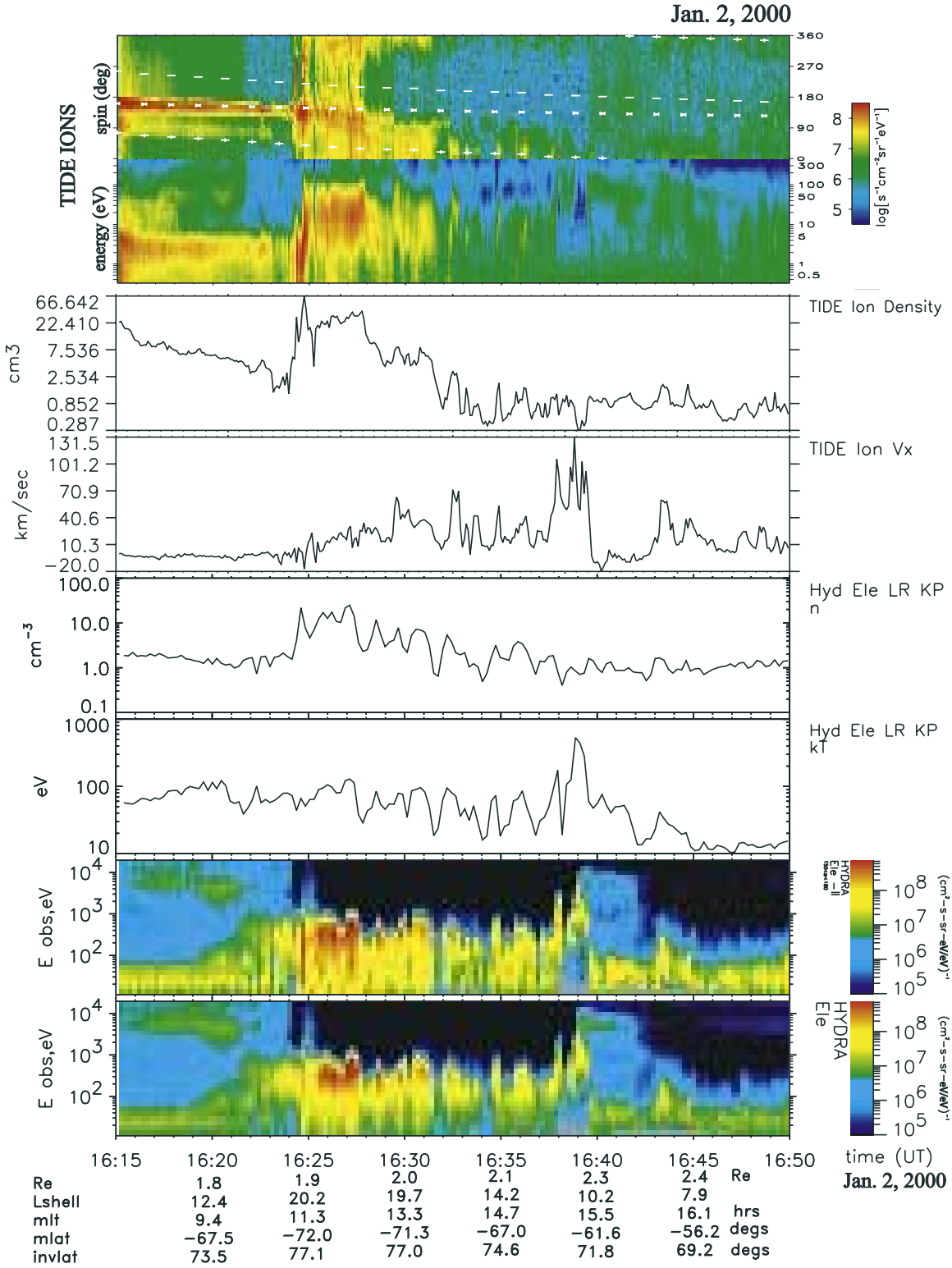

Figure 2. Top four parts are the data obtained from TIDE and the bottom four parts are from HYDRA. Shown from top to bottom are TIDE spin angle-time spectrogram, energy-time spectrogram, TIDE ion density, TIDE ion velocity along the magnetic field, electron density, electron mean energy, electron energy-time spectrogram antiparallel to the magnetic field, and the electron energy-time spectrogram including all pitch angles, respectively. This figure shows that the correlation between the ion outflow and the soft electron precipitation is substantial.

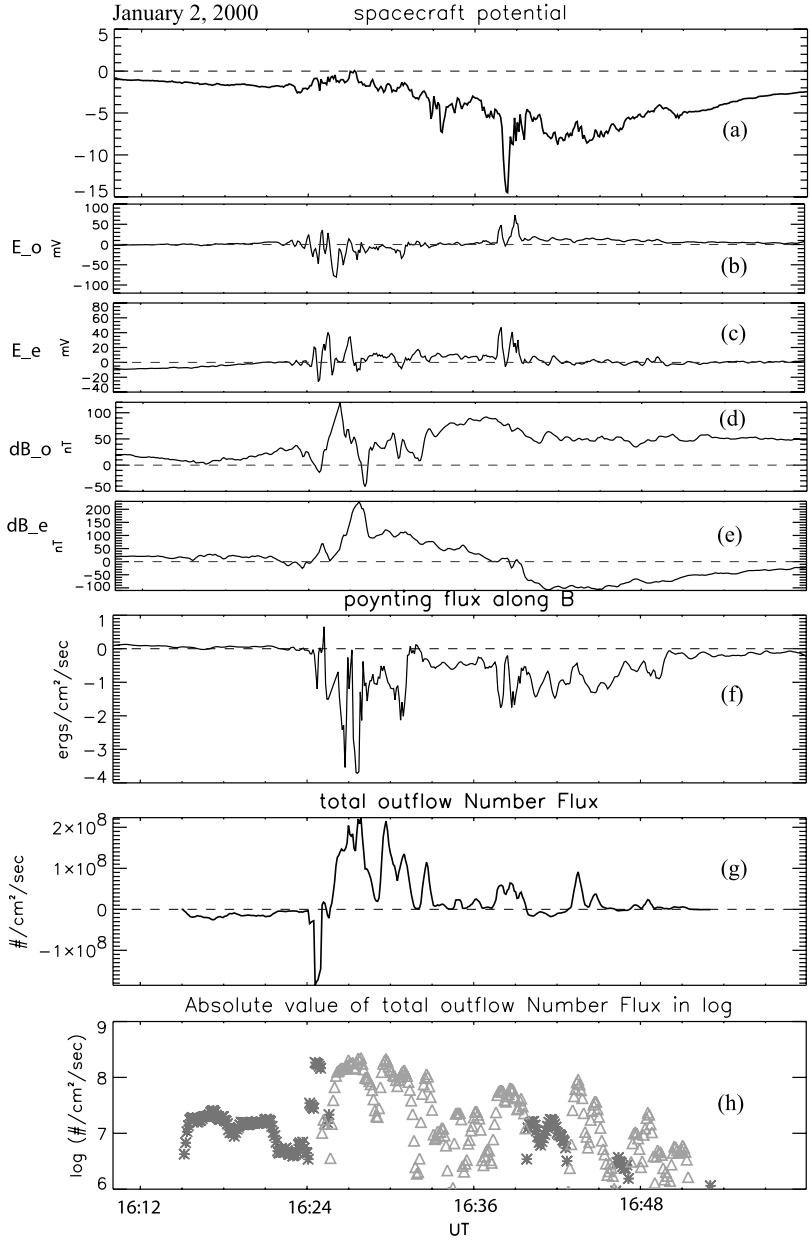

Figure 3. Polar data on 2 January 2000. (a) The spacecraft potential in volts from EFI. (b)–(e) The perturbed perpendicular electric and magnetic fields. (f) The Poynting flux along the magnetic field in ergs/cm^2/s with negative values meaning the electromagnetic energy flux going earthward. (g) The magnetic field-aligned total ion number flux obtained from TIDE in #/cm^2/s, positive values indicating outflowing ions. (h) The absolute value of total ion outflow number flux in logarithmic value, with grey triangles representing outflowing ion flux and black stars representing incoming ion flux.

flux is the energy flux in unit of keV/cm^2/s calculated from the 29 channels of differential energy fluxes.

2.3. Statistical Results

[13] After performing a thorough analysis on each individual event, we did the statistical analysis for the 37 events in the database. The results are shown in Figures 5, 6, 7, and 8.

[14] By examining the plots of the field-aligned Poynting flux versus the total field-aligned ion outflow flux of all 37 events, we find that the correlation between the two quantities is remarkable in the sense that whenever there is a nonzero Poynting flux along B, there is a corresponding nonzero total field-aligned ion outflow flux (as shown in Figure 3 for the 2 January 2000 event). Even the point by point correlation of all the data points from all the events (11,507 data points) is not bad, considering that all the data points are included without any discrimination (such as picking out those when substantial ion outflows were seen). Figure 4 shows the point by point correlation result between the field-aligned total ion outflow and the Poynting flux with the top part of their original values (the correlation coefficient: 0.42) and the bottom part of their absolute values (the correlation coefficient: 0.33).

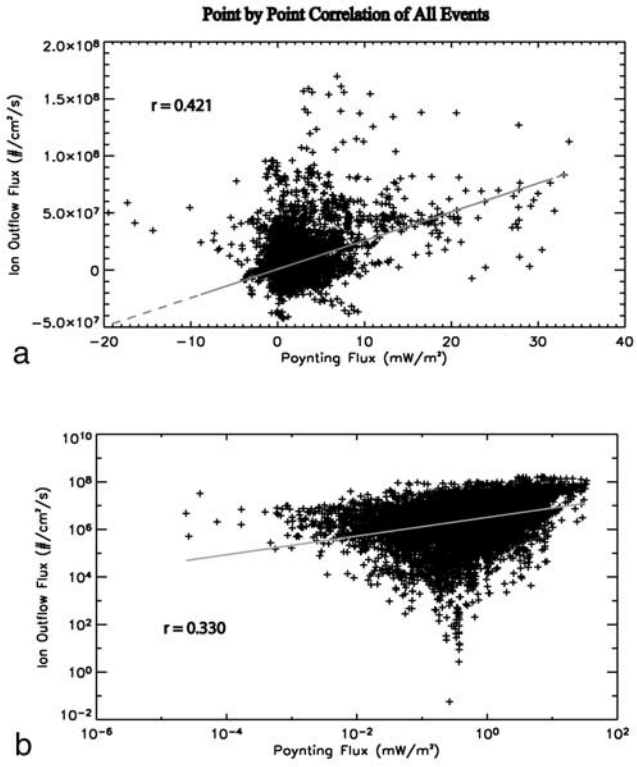

Figure 4. The point by point correlation result between the field-aligned total ion outflow and the Poynting flux with the top part of their original values and the bottom part of their absolute values. The positive *y* axis value in the top part indicates the outflowing ion flux, while the positive *x* value means the earthward flowing Poynting flux.

The positive *y* axis value in the top part indicates the outflowing ion flux, while the positive *x* value means the earthward flowing Poynting flux.

[15] In order to capture the obvious "long-term" (~30–50 min) correlation between the two quantities, it seems that we either use some kind of averaged value or an integrated value (there may be some other ways). The latter was abandoned because each event has its own time interval. The average value used in the paper is averaged over all data points of an event, not the absolute values. The other value used for the correlation analysis is the maximum value of an event. The same analysis method is performed with all the physical quantities considered here, as shown in Figures 5, 6, 7, and 8.

[16] Figure 5 shows the correlation results of total field-aligned ion outflow flux (#/cm^2/s) versus the Poynting flux (mW/m^2), with the top part showing the relation between the maximum values of the two variables and the bottom part showing the result for the averaged values from each event. The average value of an event is obtained by including all the data points. Each plus symbol in the plot represents the corresponding value of an event. The slope and the correlation coefficient are also marked on the plot. We can see that the total ion outflow flux correlates with the averaged Poynting flux pretty well (r = 0.724).

[17] Figures 6, 7, and 8 have similar format as that of Figure 5, with each of them illustrating the correlation results of the field-aligned total ion outflow flux versus different electron quantities. The correlation results between the total ion outflow flux and the electron density are shown in Figure 6. The relation between the total ion outflow flux and the total electron energy flux is shown in Figure 7. Figure 8 shows the results of the total ion outflow versus the electron temperature. Combining these results, we can see that for this set of events the total ion outflow flux correlates better with the Poynting flux. The electron density comes as the second controlling factor of the ion outflow. The total ion outflow does not correlate with the total electron energy flux and has no correlation with the electron temperature. The result here is not discrepant with what is found in the work of *Seo et al.* [1997], where the ion outflow flux correlates well with the precipitating soft electron temperature/electron energy flux based on their analysis of DE 2 data, as they were looking at the soft ($\leq$1 keV) precipitating electrons in the ionosphere, while we are looking at mostly the energetic magnetospheric electrons measured by HYDRA of Polar. The inclusion of energetic electrons probably accounts for the difference. The seemingly different result of the electron temperature in this paper may be also due to the fact that the Polar data used here were collected at higher altitudes (4000–6000 km), where the electron temperature may have a negligible effect on ion outflow, compared with their data that were obtained at lower altitudes (850–950 km).

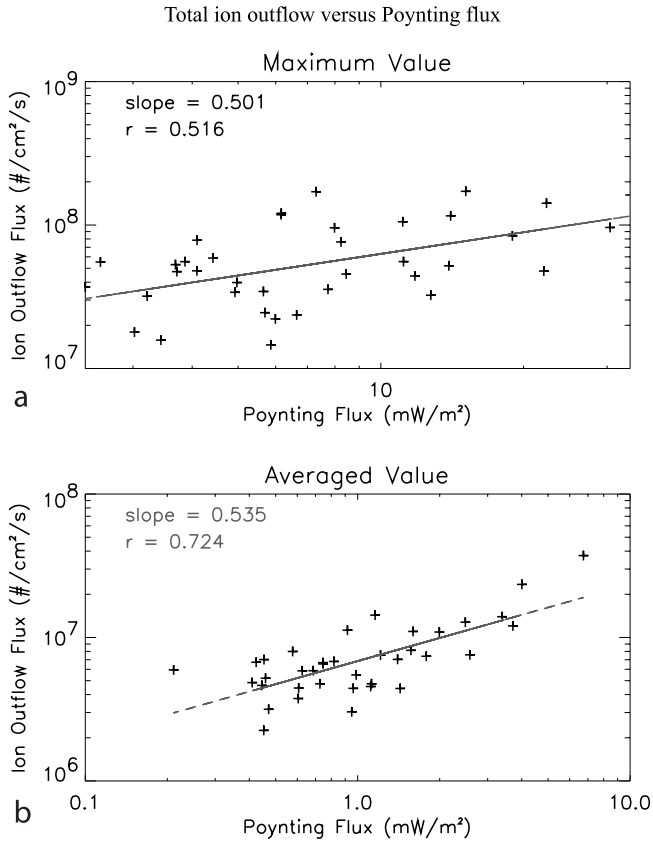

Figure 5. The statistical result of total ion outflow flux versus Poynting flux. Each plus symbol represents an event. The top part shows the correlation between the maximum values of the two quantities and the bottom part shows the correlation result between the event averages.

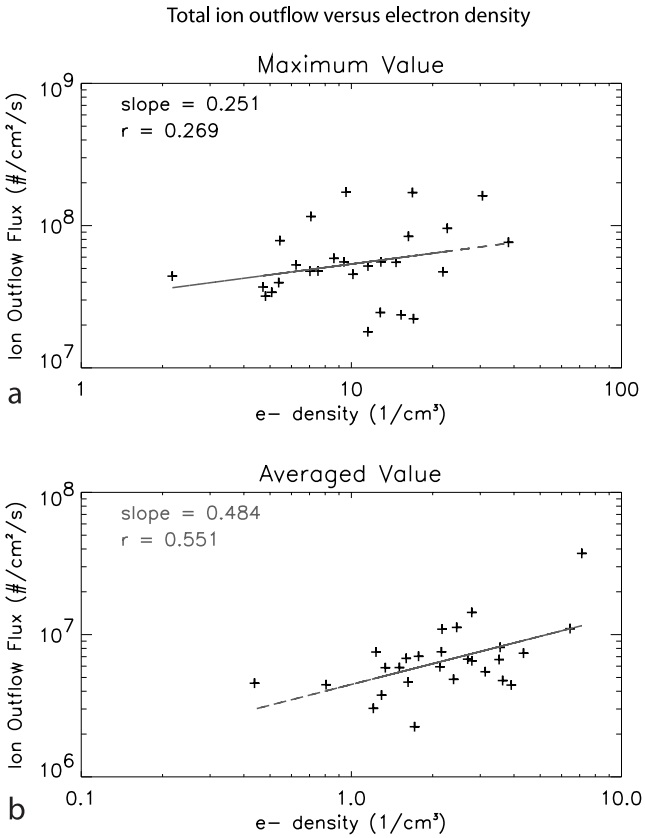

Figure 6. The statistical result of total ion outflow flux versus electron density with its format similar to Figure 5.

[18] The findings in *Strangeway et al.*'s [2005] work are that electron precipitation is the strongest average controlling factor of the ion outflow and that point by point analysis shows that Poynting flux correlates with the ion outflow better for the dayside and electron precipitation has the better correlation for the nightside. Our result is very similar to their FAST result, considering our events are mostly in the dayside. Figure 9 shows the orbit coverage for all the events of this study in terms of magnetic local time (MLT) and invariant latitude (ILAT). It should be mentioned that the orbit of the whole interval (usually ~40 min) for each ion outflow event is plotted in Figure 9. (Were only the intervals with large ion outflow flux drawn, the orbit coverage would be even more concentrated in the dayside.) Both FAST and Polar results show that dominant influences of ion outflow are Poynting flux and precipitating electron density. The general corroboration between independent data sets suggests that empirical ion outflow scaling laws can be established, which can help set the appropriate ion outflow constraint in the global simulations.

3. Discussion

[19] This statistical study concerns several factors affecting ion outflow in the dayside auroral region. Our results show that Poynting flux and precipitating electron density are the two dominant controlling factors of ion outflow, in the average sense. The Poynting flux in this study is calculated from the perturbated magnetic field and electric field, which can result from the field-aligned currents and/or Alfvén waves. (Note that Alfvén waves involved here are in the very low frequency range because of the filter [1/600–1/6 Hz] we used for the calculation.) Since there is plenty of evidence that Alfvén waves may enhance soft electron precipitation on both the dayside [e.g., *Su et al.*, 2001; *Keiling et al.*, 2003] and nightside [e.g., *Wygant et al.*, 2000; *Keiling et al.*, 2003], the two controlling factors derived from this study, Poynting flux and the precipitating electron density, are not independent of each other. Figure 1 provides a good summary of various ion outflow contributors, the ion outflow mechanisms, as well as the interrelation among them. The solid black arrow means a causal relation; the hollow black arrow means possibly causal; and the hollow grey arrow shows the two quantities are correlated. What is in black is what was observed by FAST, and the grey text shows what can be inferred based on the FAST results.

[20] Our results are very similar to the essence of the results obtained by *Strangeway et al.* [2005] using FAST data (shown in Figure 1). Figure 1 also demonstrates that the Poynting flux and the precipitating soft electrons are two very important factors controlling ion outflow. Auroral particle acceleration and the corresponding ion escape are the result of the transmission of electromagnetic energy (carried by the Poynting flux) from the magnetosphere along auroral field lines and its dissipation in the auroral acceleration region. The Poynting flux will be converted to heat in the ionosphere through Joule dissipation. This dissipation is mediated by ion-neutral collisions. Besides heating the neutrals, some of the dissipation will convert the ion flows into ion thermal energy. On the basis of *Banks*

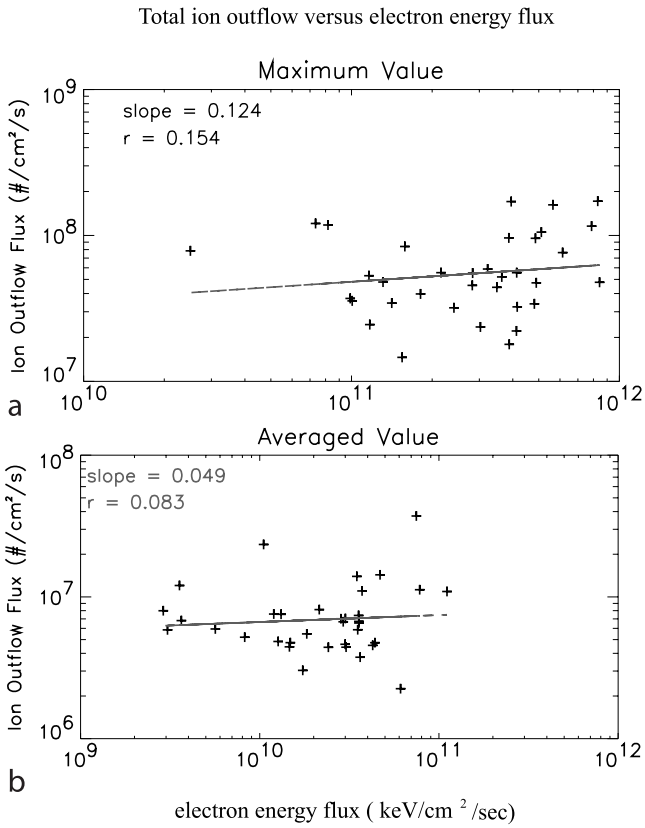

Figure 7. The statistical result of total ion outflow flux versus electron energy flux with its format similar to Figure 5.

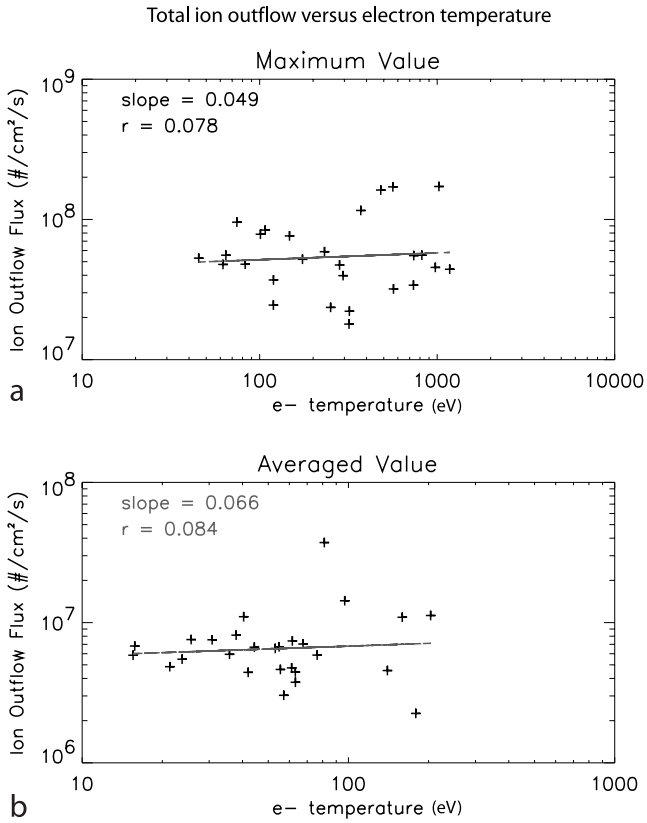

Figure 8. The statistical result of total ion outflow flux versus electron temperature with its format similar to Figure 5.

and Kockarts [1973], the Joule dissipation heats the ions in the ionosphere, and the resulting increase in ionospheric scale height will increase the column density of ions at altitudes where transverse heating occurs. At even higher altitudes, additional acceleration may also occur, such as the centrifugal acceleration [*Cladis*, 1986]. Thus the electromagnetic energy flux in the form of Poynting flux is not the sole cause for the ion outflows, but it is the necessary first step [*Strangeway et al.*, 2000].

[21] Soft electron precipitation (<1 keV) has a more immediate impact on the ion outflow than the precipitating energetic electrons. Energetic precipitating electrons deposit energy below the *F* peak (~120–200 km). While this creates ionization and heats the electron gas, the plasma is collision dominated [*Gombosi and Killeen*, 1987] so direct energy input has minimal immediate impact on the topside *F* region plasma. It takes some time (>20 min) for this energy input to affect the topside *F* region. In contrast, low-energy electron precipitation deposits considerable energy into ionospheric electrons in the *F* region and topside up to the exobase (about 500 km). This effect enhances the ambipolar electric field, raises ionospheric scale heights, and accelerates light ion outflows [e.g., *Liu et al.*, 1995; *Horwitz and Moore*, 1997]. In addition, fast auroral plasma winds of a few kilometers per second experience ion-neutral friction that heats heavy ions strongly by ionospheric standards, increasing scale heights and producing an extended topside ionosphere [*Heelis et al.*, 1993; *Loranc et al.*, 1991]. This direct scale height increase from energy input at or near the exobase results in an upward flow of ions from the ionosphere, which may result in escape if higher-altitude heating is present.

[22] Ionospheric ion outflows are not just important in providing a significant plasma source for the magnetosphere (there have been observational results showing that O+ can be present in the midtail lobe/mantle and distant tail [e.g., *Seki et al.*, 1996]) but have a clear role in controlling the global dynamics of the magnetosphere and the transport of the solar wind energy and momentum through magnetosphere. Using a multifluid MHD model, *Winglee et al.* [2002] demonstrated that the presence of heavy ionospheric outflows has macroscopic effects on the global dynamics of the magnetosphere, including limiting the cross-polar cap potential, providing a substantial energy sink for the energy flowing into the auroral region, modifying the open/closed boundary, and determining the distribution of energetic particles in the magnetosphere. The mass loading, resulting from the ionospheric ion outflows, into the magnetotail may have effects on the reconnection rate, reconnection structure, the occurrence of substorms, and so on. Advances in understanding the global impact of the ionospheric ion outflows require a testable self-consistent outflow model within the GGCM. This work serves as a step toward that direction and will be of help in setting the proper inner boundary and right constraint.

4. Conclusion

[23] A statistical study of ionospheric ion outflow versus its energy inputs was performed using Polar data. The database of the study is composed of 37 ion outflow events (mostly in the dayside) during Polar's auroral perigee passes in the year 2000. Poynting flux due to Alfvén waves and/or field-aligned currents and precipitating electron density were found to be the two dominant controlling factors of ion outflow. The results from Polar are very similar to those of FAST. The general corroboration between the independent data sets

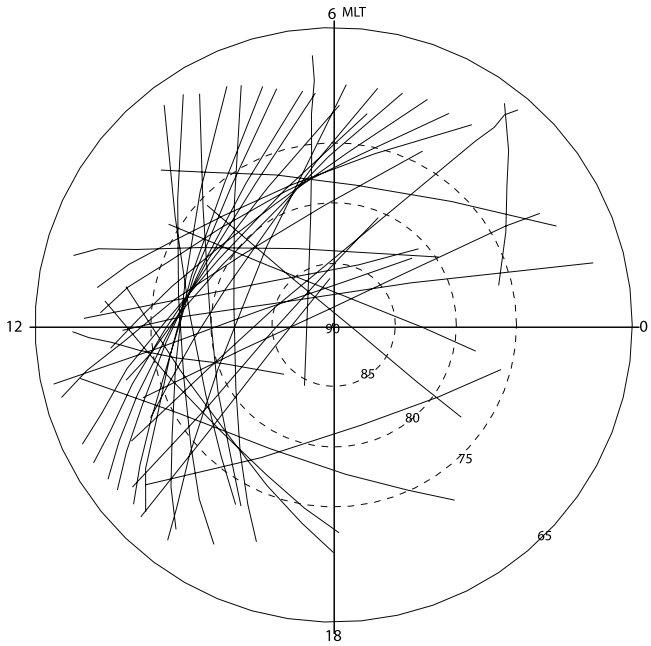

Figure 9. The orbit coverage for all the events in the database in terms of magnetic local time (MLT) and invariant latitude.

suggests that empirical ion outflow scalings can be established. Our results show that at 6000 km altitudes $f_i = 10^{6.836\pm0.028}S^{0.535\pm0.086}$ and $f_i = 10^{6.650\pm0.063}n_e^{0.484\pm0.147}$ (f_i: the total field-aligned ion outflow flux in $1/cm^2/s$; S: field-aligned Poynting flux in $ergs/cm^2/s$; and n_e: the electron density in $1/cm^3$). The above statistical relations are obtained using the averaged values of all the events. The difference between the results here and those by *Strangeway et al.* [2005] may arise from the fact that we used all the ion outflow events during the year 2000 while their results were derived using data acquired from 33 FAST orbits during the 24–25 September 1998 storm time only. The different ways of getting n_e may contribute to the difference as well.

[24] The results from the two studies can serve as guidance for setting up the proper global simulation boundary conditions and for the full theory development of auroral response in the ionosphere-thermosphere-magnetosphere (ITM) coupling community. Of course, in order to reach the ultimate goal of having a testable self-consistent outflow model, more statistical studies of this type are needed.

[25] **Acknowledgments.** We would like to thank Philip Valek, Craig Pollock at Southwest Research Institute, and Peggy Sloan at NASA Marshall Space Flight Center for the assistance with TIDE software. We are grateful to both reviewers for their substantive and constructive comments.

[26] Arthur Richmond thanks Yi-Jiun Su and Andrew Yau for their assistance in evaluating this paper.

References

Banks, P. M., and G. Kockarts (1973), *Aeronomy, Part B*, Elsevier, New York.

Cannata, R. W., and T. I. Gombosi (1989), Modeling of the solar cycle dependence of quiet-time ion upwelling at high geomagnetic latitudes, *Geophys. Res., Lett.*, *16*, 1141.

Chappell, C. R., T. E. Moore, and J. H. Waite Jr. (1987), The ionosphere as a fully adequate source of plasma for the Earth's magnetosphere, *J. Geophys. Res.*, *92*, 5896.

Chappell, C. R., B. L. Giles, T. E. Moore, D. C. Delcourt, P. D. Craven, and M. O. Chandler (2000), The adequacy of the ionospheric source in supplying magnetospheric plasma, *J. Atmos. Sol. Terr. Phys.*, *62*, 421.

Chaston, C. C., C. W. Carlson, W. J. Peria, and R. E. Ergun (1999), FAST observations of inertial Alfvén waves in the dayside aurora, *Geophys. Res. Lett.*, *26*, 647.

Chaston, C. C., J. W. Bonnell, C. W. Carlson, J. P. McFadden, R. E. Ergun, and R. J. Strangeway (2003), Properties of small-scale Alfvén waves and accelerated electrons from FAST, *J. Geophys. Res.*, *108*(A4), 8003, doi:10.1029/2002JA009420.

Chen, S.-H., and T. E. Moore (2004), Dayside flow bursts in the Earth's outer magnetosphere, *J. Geophys. Res.*, *109*, A03215, doi:10.1029/2003JA010007.

Cladis, J. B. (1986), Parallel acceleration and transport of ions from polar ionosphere to plasma sheet, *Geophys. Res. Lett.*, *13*, 893.

Collin, H. L., W. K. Peterson, O. W. Lennartsson, and J. F. Drake (1998), The seasonal variation of auroral ion beams, *Geophys. Res. Lett.*, *25*, 4071.

Fuselier, S. A., et al. (2001), Ion outflow observed by IMAGE: Implications for source region and heating mechanism, *Geophys. Res. Lett.*, *28*, 1163.

Giles, B. L. (1993), Inner magnetosphere circulation of thermal ions inferred from observed pitch angle distributions, Ph.D. thesis, Univ. of Alabama, Huntsville, Ala.

Gombosi, T. I., and T. L. Kileen (1987), Effects of thermospheric motions of the polar wind: A time-dependent numerical study, *J. Geophys. Res.*, *92*, 4725.

Harvey, P., et al. (1995), The electric field measurement on the Polar satellite, *Space Sci. Rev.*, *71*, 583.

Heelis, R. A., R. G. J. Bailey, R. Sellek, R. J. Moffett, and B. Jenkins (1993), Field-aligned drifts in subauroral ion drift events, *J. Geophys. Res.*, *98*, 21,493.

Horwitz, J. L., and T. E. Moore (1997), Four contemporary issues concerning ionospheric plasma flow to the magnetosphere, *Space Sci, Rev.*, *80*, 49.

Keiling, A., J. R. Wygant, C. A. Cattell, F. S. Mozer, and C. T. Russell (2003), The global morphology of wave Poynting flux: Powering the aurora, *Science*, *299*(5605), 383.

Liu, C., J. L. Horwitz, and P. G. Richards (1995), Effects of frictional ion heating and soft electron precipitation on high-latitude *F* region upflows, *Geophys. Res. Lett.*, *22*, 2713.

Loranc, M., W. B. Hanson, R. A. Heelis, and J.-P. St.-Maurice (1991), A morphological study of vertical ionospheric flows in the high-latitude F region, *J. Geophys. Res.*, *96*, 3627.

Moore, T. E. (1991), Origins of magnetospheric plasma, *Rev. Geophys.*, *29*, 1039.

Moore, T. E., and D. C. Delcourt (1995), The geopause, *Rev. Geophys*, *33*, 175.

Moore, T. E., et al. (1995), The thermal ion dynamics experiment and plasma source instrument, *Space Sci. Rev.*, *71*(1-4), 409.

Moore, T. E., W. K. Peterson, C. T. Russell, M. O. Chandler, M. R. Collier, H. L. Collin, P. D. Craven, R. Fitzenreiter, B. L. Giles, and C. J. Pollock (1999), Ionospheric mass ejection in response to a CME, *Geophys. Res. Lett.*, *26*, 2339.

Pollock, C. J., M. O. Chandler, T. E. Moore, J. H. Waite Jr., C. R. Chappell, and D. A. Gurnett (1990), A survey of upwelling ion event characteristics, *J. Geophys. Res.*, *95*, 18,969.

Russell, C. T., R. C. Snare, J. D. Means, D. Pierce, D. Dearborn, M. Larson, G. Barr, and G. Le (1995), The GGS/Polar magnetic fields investigation, in *The Global Geospace Mission*, edited by C. T. Russell, p. 563, Springer, New York.

Scudder, J. D., et al. (1995), Hydra—A three dimensional electron and ion instrument for the Polar spacecraft of the GGS mission, *Space Sci. Rev.*, *71*, 459.

Seki, K., M. Hirahara, T. Terasawa, I. Shinohara, T. Mukai, Y. Saito, S. Machida, T. Yamamoto, and S. Kokubun (1996), Coexistence of Earth-origin O+ and solar wind-origin H+/He++ in the distant magnetotail, *Geophys. Res. Lett.*, *23*, 985.

Seo, Y., J. L. Horwitz, and R. Caton (1997), Statistical relationships between high-latitude ionospheric *F* region/topside upflows and their drivers: DE 2 observations, *J. Geophys. Res.*, *102*, 7493.

Strangeway, R. J., C. T. Russell, C. W. Carlson, J. P. McFadden, R. E. Ergun, M. Temerin, D. M. Klumpar, W. K. Peterson, and T. E. Moore (2000), Cusp field-aligned currents and ion outflows, *J. Geophys. Res.*, *105*, 21,129.

Strangeway, R. J., R. E. Ergun, Y.-J. Su, C. W. Carlson, and R. C. Elphic (2005), Factors controlling ionospheric outflows as observed at intermediate altitudes, *J. Geophys. Res.*, *110*, A03221, doi:10.1029/2004JA010829.

Su, Y.-J., R. E. Ergun, W. K. Peterson, T. G. Onsager, R. Pfaff, C. W. Carlson, and R. J. Strangeway (2001), Fast Auroral Snapshot observations of cusp electron and ion structures, *J. Geophys. Res.*, *106*, 25,595.

Tung, Y.-K., C. W. Carlson, J. P. McFadden, D. M. Klumpar, G. K. Parks, W. J. Peria, and K. Liou (2001), Auroral polar cap boundary ion conic outflow observed on FAST, *J. Geophys. Res.*, *106*, 3603.

Winglee, R. M. (1998), Multi-fluid simulations of the magnetosphere: The identification of the geopause and its variation with IMF, *Geophys. Res. Lett.*, *25*, 4441.

Winglee, R. M. (2004), Ion cyclotron and heavy ion effects on reconnection in a global magnetotail, *J. Geophys. Res.*, *109*, A09206, doi:10.1029/2004JA010385.

Winglee, R. M., D. Chua, M. Brittnacher, G. K. Parks, and G. Lu (2002), Global impact of ionospheric outflows on the dynamics of the magnetosphere and cross-polar cap potential, *J. Geophys. Res.*, *107*(A9), 1237, doi:10.1029/2001JA000214.

Wygant, J. R., et al. (2000), Polar spacecraft based comparisons of intense electric fields and Poynting flux near and within the plasma sheet-tail lobe boundary to UVI images: An energy source for the aurora, *J. Geophys. Res.*, *105*, 18,675.

Yau, A. W., and M. André (1997), Sources of ion outflow in the high latitude ionosphere, *Space Sci. Rev.*, *80*, 1.

Yau, A. W., E. G. Shelley, W. K. Peterson, and L. Lenchyshyn (1985), Energetic auroral and polar ion outflow at DE-1 altitudes: Magnitude, composition, magnetic activity dependence and long-term variations, *J. Geophys. Res.*, *90*, 8417.

T. E. Moore, Laboratory for Extraterrestrial Physics, NASA Goddard Space Flight Center, Greenbelt, MD 20771, USA. (thomas.e.moore@nasa.gov)

F. S. Mozer, Space Science Laboratory, University of California at Berkeley, Berkeley, CA 94720, USA. (mozer@ssl.berkeley.edu)

C. T. Russell and R. J. Strangeway, Institute of Geophysics and Planetary Physics, University of California at Los Angeles, Los Angeles, CA 90024-1567, USA. (ctrussell@igpp.ucla.edu; strange@igpp.ucla.edu)

Y. Zheng, Johns Hopkins University Applied Physics Laboratory, Laurel, MD 20723, USA. (yihua.zheng@jhuapl.edu)